Journal of Electron Spectroscopy and Related Phenomena 211 (2016) 41–46

Contents lists available at ScienceDirect

Journal of Electron Spectroscopy and Related Phenomena

journal homepage: www.elsevier.com/locate/elspec

Calculation of Franck–Condon factors and simulation of photoelectron spectra of the $HCCl^-$ anion: Including Duschinsky effects

Zhen-li Yang[a], Zhou Zhang[b], Shuai Jiang[b], Ya-juan Feng[b], Jun Liang[a,**], Wei Huang[b,*]

[a] Institute of Atomic and Molecular Physics, College of Physics and Electronic Information, Anhui Normal University, Wuhu 241000, PR China
[b] Laboratory of Atmospheric Physic-Chemistry, Anhui Institute of Optics & Fine Mechanics, Chinese Academy of Sciences, Hefei, Anhui 230031, PR China

ARTICLE INFO

Article history:
Received 23 December 2015
Received in revised form 3 June 2016
Accepted 3 June 2016
Available online 8 June 2016

Keywords:
Spectral simulation
Duschinsky effects
Hot band

ABSTRACT

Halomethylenes (such as HCCl) are particularly critical intermediates in many gas-phase reaction environments. The structures, spectra, and reactivity of environment-related molecules have been of many studies interest. In the present work, geometry optimization and frequency calculations have been carried out on the $\tilde{X}^2A''$ state of $HCCl^-$ and the $\tilde{X}^1A'$ and $\tilde{a}^3A''$ states of HCCl at CCSD(T) theory. The single point energy, electron affinity and term energy of HCCl have been computed up to the CCSD(T)/aug-cc-pV5Z level and extrapolated to the complete basis set limit. The Duschinsky matrix and displacement vector have been considered at the CCSD(T) level of theory and the result shows that the normal mode mixing effects play a main role for $HCCl(\tilde{a}^3A'')$–$HCCl^-(\tilde{X}^2A'')$ transition, and which can be neglected for the $HCCl(\tilde{X}^1A')$–$HCCl^-(\tilde{X}^2A'')$ process. Franck–Condon analysis and spectral simulations have been performed on the singlet and triplet photo-detachment processes, respectively. We have merged the singlet and triplet transitions together for the first time and the results show that the simulated spectra are very consistent with the previous experimental one.

© 2016 Elsevier B.V. All rights reserved.

1. Introduction

Currently, the quality of the atmospheric environment has deteriorated due to people and economic activities as well as a growing vehicle fleet, this deeply affected the daily lives and health of millions of people [1–5]. The structures, spectra, and reactivity of environment-related molecules have been the subjection of many theoretical and experimental researches [6–24]. Halomethylenes (such as HCCl) are important reactive intermediates in many gas-phase reaction environments, such as atmospheric chemistry [23,25,26]. The subject of the present paper is to investigate the photoelectron spectra of $HCCl^-$ theoretically through the Franck–Condon factor calculations in the spectral simulations.

In the early study, Merer and Travis have published the observed visible and near-infrared (IR) spectra of the $\tilde{A}^1A''$–$\tilde{X}^1A'$ electronic transition of HCCl and assigned the band system in the region 5500 and 8200 Å [27]. Following this pioneering work, a number of spectroscopic studies on the $\tilde{A}$–$\tilde{X}$ transition have been published both in the argon matrix [28] and in gas phase [17,19,29–34]. Considering that the $\tilde{X}^1A'$ and $\tilde{a}^3A''$ states of HCCl are very close in energy but have significant difference in chemistries, the high precision measurement of the singlet–triplet energy gap (term energy) is vital to understand the reaction mechanisms [10,23,35]. In the present work, the term energy calculated at the CCSD(T) level of theory with Dunning's correlation consistent basis sets and extrapolated to the complete basis set limit, which have been compared with the previous experimental results.

Most studies are centered on the neutral molecules HCCl [8–10,12,19–23,36–39], and its corresponding negative ion $HCCl^-$ comparatively sparse [7,13,14,40,41]. The photoelectron spectroscopy (PES) of $HCCl^-$ has been studied by Lineberger et al. [40,41], which was used to investigate the electron affinity of the HCCl molecule and geometries and frequencies of the HCCl and $HCCl^-$ molecules. In order to confirm their origin assignments, Franck–Condon factors (FCFs) for the $HCCl(\tilde{X}^1A')$–$HCCl^-(\tilde{X}^2A'')$ transition have been calculated without taking into account the Duschinsky effects [42] in the two works. In 2012 [13], Zhang et al. reported the theoretical PES of the $HCCl(\tilde{X}^1A')$–$HCCl^-(\tilde{X}^2A'')$ including Duschinsky effects. Nevertheless, they disregarded hot bands in the FCF analysis totally, and did not theoretically investi-

* Corresponding author at: Laboratory of Environment Spectroscopy, Anhui Institute of Optics and Fine Mechanics, Chinese Academy of Sciences, P.O. Box 1125, Hefei 230031, PR China.
** Corresponding author. Fax: +86 0553 3869 748.
E-mail addresses: jliang@mail.ahnu.edu.cn (J. Liang), huangwei@aiofm.ac.cn (W. Huang).

http://dx.doi.org/10.1016/j.elspec.2016.06.003
0368-2048/© 2016 Elsevier B.V. All rights reserved.

Table 1
Comparison of the theoretical and experimental geometries and vibrational frequencies for the $\tilde{X}^2A''$ state of $HCCl^-$ obtained at different levels. Bond lengths, angles and frequencies are given in angstroms, degrees and cm^{-1}, respectively.

Method	R(C—H)	R(C—Cl)	∠HCCl	ω_1(CH)	ω_2(bend)	ω_3(CCl)
CCSD(T)/cc-pVDZ	1.1511	1.9941	94.25	2651	1094	445
CCSD(T)/cc-pVTZ	1.1249	1.9466	95.15	2725	1118	468
CCSD(T)/cc-pVQZ	1.1215	1.9249	95.82	2751	1127	474
CCSD(T)/cc-pV5Z	1.119	1.9067	96.53	2772	1129	484
CCSD(T)/aug-cc-pVDZ	1.1397	1.9749	95.57	2725	1084	431
CCSD(T)/aug-cc-pVTZ	1.1206	1.9229	96.52	2767	1115	472
CCSD(T)/aug-cc-pVQZ	1.1191	1.9076	96.80	2775	1123	480
CCSD(T)/aug-cc-pV5Z	1.1184	1.8982	96.98	2779	1126	485
IFCA[a]		1.950 ± 0.002				
Expt.[b]	1.14 ± 0.02	1.91 ± 0.02	99.5 ± 3			445 ± 25
Expt.[c]	1.12 ± 0.02	1.99 ± 0.02	96 ± 0.02			470 ± 30

[a] Ref. [13].
[b] Ref. [41].
[c] Ref. [40].

gate how the hot bands overlap with the cold ones and bring about the final spectral pattern is unsure.

Based on those researches, we further explore the PES of the singlet $HCCl(\tilde{X}^1A')$–$HCCl^-(\tilde{X}^2A'')$ and triplet $HCCl(\tilde{a}^3A'')$–$HCCl^-(\tilde{X}^2A'')$ transitions theoretically including the Duschinsky effects and hot bands. Geometry optimization and frequency calculations have been performed on the $\tilde{X}^2A''$ state of $HCCl^-$, and the $\tilde{X}^1A'$ and $\tilde{a}^3A''$ states of HCCl. Single point energy, electron affinity and term energy were acquired by CCSD(T) level with Dunning's correlation consistent basis sets and extrapolated to the complete basis set limit using a two-parameter mixed GAUSSIAN function [43]. The Duschinsky matrix and displacement vector have been derived at the CCSD(T)/aug-cc-pV5Z level. Franck–Condon analysis and spectral simulations were carried out on the singlet $\tilde{X}^1A'$–$\tilde{X}^2A''$ and triplet $\tilde{a}^3A''$–$\tilde{X}^2A''$ transitions. The singlet and triplet electronic transitions of $HCCl^-$ are merged together for the first time, which could compare better with the experimental spectra.

2. Calculation method of Franck–Condon factors

The normal coordinates of electronic states not only undergo a displacement distortion but also a rotation on an electronic transition. The normal coordinate rotation results in a normal mode mixing and thereby the non-separability of the multidimensional Franck–Condon (FC) integrals. In 1937, Duschinsky [42] proposed the transformation relationship between the normal coordinates of the initial ($\mathbf{Q}'$) and the final ($\mathbf{Q}''$) electronic states

$$\mathbf{Q}' = \mathbf{J}\mathbf{Q}'' + \mathbf{K} \tag{1}$$

Here $\mathbf{K}$ is a vector whose components are the changes in the nuclear equilibrium positions from the initial to final states and $\mathbf{J}$ is a constant orthogonal matrix that evaluates the normal mode mixing effects. It has been shown that the relationship is most generally neither linear nor orthogonal between the vibrational variables for two different electronic states of a polyatomic molecule [44]. However, in quantitative studies on the basis of the FC principle, the linear–orthogonal transformation, Eq. (1), is widely accepted.

To investigate the non-radiative processes and clarify vibronic spectra of molecules, it is very important to calculate Franck–Condon factors (the square of the vibrational overlap integrals). A lot of theoretical methods have been proposed to evaluate the multidimensional FC integrals quantitatively [45–54]. Recently, on the basis of the harmonic oscillator approximation including the Duschinsky effects, a more general expression has been derived by our study group [55]. For the vibronic transition $|\upsilon_1\upsilon_2\upsilon_3\rangle \longleftarrow |\upsilon'_1\upsilon'_2\upsilon'_3\rangle$, Franck–Condon integral $\langle\upsilon_1\upsilon_2\upsilon_3|\upsilon'_1\upsilon'_2\upsilon'_3\rangle$ are expressed as

$$\begin{aligned}
\langle\upsilon_1\upsilon_2\upsilon_3|\upsilon'_1\upsilon'_2\upsilon'_3\rangle = {} & \exp\left(-\frac{1}{2}\mathbf{K}^{+}\boldsymbol{\Gamma}'\mathbf{K}\right)\exp\left(\mathbf{C}^{+}\mathbf{A}\mathbf{C}\right)\mathrm{N} \\
& \times \sum_{k'_{11}=0}^{\upsilon'_1}\sum_{k'_{12}=0}^{\upsilon'_1-k'_{11}}\sum_{k'_{13}=0}^{\upsilon'_1-k'_{11}-k'_{12}}\sum_{k'_{21}=0}^{\upsilon'_2}\sum_{k'_{22}=0}^{\upsilon'_2-k'_{21}}\sum_{k'_{23}=0}^{\upsilon'_2-k'_{21}-k'_{22}}\sum_{k'_{31}=0}^{\upsilon'_3}\sum_{k'_{32}=0}^{\upsilon'_3-k'_{31}}\sum_{k'_{33}=0}^{\upsilon'_3-k'_{31}-k'_{32}} \\
& \sum_{k_{11}=0}^{\upsilon_1}\sum_{k_{12}=0}^{\upsilon_1-k_{11}}\sum_{k_{13}=0}^{\upsilon_1-k_{11}-k_{12}}\sum_{k_{21}=0}^{\upsilon_2}\sum_{k_{22}=0}^{\upsilon_2-k_{21}}\sum_{k_{23}=0}^{\upsilon_2-k_{21}-k_{22}}\sum_{k_{31}=0}^{\upsilon_3}\sum_{k_{32}=0}^{\upsilon_3-k_{31}}\sum_{k_{33}=0}^{\upsilon_3-k_{31}-k_{32}} \\
& \left\{\prod_{i=1}^{3}\left[\binom{\upsilon'_i}{k'_{i1}}\binom{\upsilon'_i-k'_{i1}}{k'_{i2}}\binom{\upsilon'_i-k'_{i1}-k'_{i2}}{k'_{i3}}\right.\right. \\
& \times (a'_{i1})^{k'_{i1}}(a'_{i2})^{k'_{i2}}(a'_{i3})^{k'_{i3}} \times H_{\upsilon'_i-k'_{i1}-k'_{i2}-k'_{i3}}(d'_i) \\
& \times \binom{\upsilon_i}{k_{i1}}\binom{\upsilon_i-k_{i1}}{k_{i2}}\binom{\upsilon_i-k_{i1}-k_{i2}}{k_{i3}} \\
& \left.\left.\times (2a_{i1})^{k_{i1}}(2a_{i2})^{k_{i2}}(2a_{i3})^{k_{i3}} \times H_{\upsilon_i-k_{i1}-k_{i2}-k_{i3}}(d_i)\right]\right. \\
& \times \frac{[\sum_{i=1}^{3}(k_{i1}+k'_{i1})-1]!!}{\frac{1}{2}\sum_{i=1}^{3}(k_{i1}+k'_{i1})}\left(\frac{\pi}{A_1}\right)^{1/2}\frac{[\sum_{i=1}^{3}(k_{i2}+k'_{i2})-1]!!}{\frac{1}{2}\sum_{i=1}^{3}(k_{i2}+k'_{i2})}\left(\frac{\pi}{A_2}\right)^{1/2} \\
& \times \frac{[\sum_{i=1}^{3}(k_{i3}+k'_{i3})-1]!!}{\frac{1}{2}\sum_{i=1}^{3}(k_{i3}+k'_{i3})}\left(\frac{\pi}{A_3}\right)^{1/2}\Bigg\}
\end{aligned} \tag{2}$$

with the constraints that $\sum_{i=1}^{3}(k_{i1}+k'_{i1})$, $\sum_{i=1}^{3}(k_{i2}+k'_{i2})$ and $\sum_{i=1}^{3}(k_{i3}+k'_{i3})$ are even. In Eq. (2), $\mathbf{K}$ is a 3×1 vector whose components are the changes in the nuclear equilibrium positions from the initial to final states and $\boldsymbol{\Gamma}'$ is a 3×3 diagonal matrix of reduced frequency $\omega'_i/\hbar$, and $\mathbf{A}$ is also a 3×3 diagonal matrix and $\mathbf{C}$ is a 3×1 vector whose elements and the other coefficients are given in Ref. [55]. Furthermore, the Franck–Condon factors can be calculated by

$$\mathrm{FCFs} = |\langle\upsilon_1\upsilon_2\upsilon_3|\upsilon'_1\upsilon'_2\upsilon'_3\rangle|^2 \tag{3}$$

Eq. (2) is very useful for studying vibronic spectra and non-radiative processes of molecules.

Table 2
Comparison of the theoretical and experimental geometries and vibrational frequencies for the singlet state ($\tilde{X}^1A'$) of HCCl obtained at different levels. Bond lengths, angles and frequencies are given in angstroms, degrees and cm^{-1}, respectively.

Method	R(C—H)	R(C—Cl)	∠HCCl	ω_1(CH)	ω_2(bend)	ω_3(CCl)
CCSD(T)/cc-pVDZ	1.1287	1.7261	101.36	2899	1222	812
CCSD(T)/cc-pVTZ	1.1104	1.7063	101.81	2912	1224	816
CCSD(T)/cc-pVQZ	1.1088	1.6983	102.01	2923	1227	822
CCSD(T)/cc-pV5Z	1.1082	1.6928	102.15	2927	1226	826
CCSD(T)/aug-cc-pVDZ	1.1270	1.7311	101.36	2889	1218	791
CCSD(T)/aug-cc-pVTZ	1.1103	1.7056	101.95	2914	1223	811
CCSD(T)/aug-cc-pVQZ	1.1087	1.6977	102.14	2926	1227	822
CCSD(T)/aug-cc-pV5Z	1.1082	1.6927	102.27	2928	1226	825
CCSD(T)/aug-cc-pVQZ[a]				2924	1223	821
CCSD(T)/cc-pVTZ[b]	1.111	1.707	101.8	2919	1229	831
Expt.[c]	1.130 ± 0.036	1.687 ± 0.011	105.1 ± 4.7			
Expt.[d]	1.1002 ± 0.0011	1.69254 ± 0.00021	102.669 ± 0.070			
Expt.[e]				2942 ± 7	1229 ± 2	830 ± 2
Expt.[f]						810 ± 25

[a] Ref. [10].
[b] Ref. [9].
[c] Ref. [29].
[d] Ref. [39].
[e] Ref. [20].
[f] Ref. [41].

Table 3
Comparison of the theoretical and experimental geometries and vibrational frequencies for the triplet state ($\tilde{a}^3A''$) of HCCl obtained at different levels. Bond lengths, angles and frequencies are given in angstroms, degrees and cm^{-1}, respectively.

Method	R(C—H)	R(C—Cl)	∠HCCl	ω_1(CH)	ω_2(bend)	ω_3(CCl)
CCSD(T)/cc-pVDZ	1.0993	1.6911	125.73	3203	984	882
CCSD(T)/cc-pVTZ	1.0824	1.6701	126.24	3203	979	888
CCSD(T)/cc-pVQZ	1.0814	1.6621	126.29	3207	974	895
CCSD(T)/cc-pV5Z	1.0813	1.6562	126.34	3207	975	900
CCSD(T)/aug-cc-pVDZ	1.0982	1.6948	125.55	3180	973	868
CCSD(T)/aug-cc-pVTZ	1.0830	1.6699	126.11	3198	970	884
CCSD(T)/aug-cc-pVQZ	1.0818	1.6625	126.20	3203	975	893
CCSD(T)/aug-cc-pV5Z	1.0812	1.6572	126.32	3207	971	896
CCSD(T)/aug-cc-pVQZ[a]				3203	970	893
CCSD(T)/cc-pVTZ[b]	1.083	1.671	126.3	3229	985	905
Expt.[c]				3083 ± 5	972 ± 4	886 ± 4
Expt.[d]						850 ± 60

[a] Ref. [10].
[b] Ref. [9].
[c] Ref. [20].
[d] Ref. [41].

Table 4
Single point energy with the ZPE correction of the $\tilde{X}^2A''$ state of $HCCl^-$ and the $\tilde{X}^1A'$ and $\tilde{a}^3A''$ states of HCCl, as well as the electron affinity and term energy were determined and extrapolated to the complete basis set limit. The experimental and theoretical values are included for comparison. Single point energy, electron affinity and term energy are given in Hartree, eV and cm^{-1}, respectively.

X	Method	$HCCl^-$	HCCl(s)	HCCl(t)	EA	TE
3	CCSD(T)/cc-pVTZ	−498.23928	−498.20569	−498.19636	0.914	2047.70
4	CCSD(T)/cc-pVQZ	−498.28055	−498.24019	−498.23031	1.098	2168.41
5	CCSD(T)/cc-pV5Z	−498.29506	−498.25180	−498.24180	1.177	2194.75
∞	CBS-3parameter	−498.30349	−498.25864	−498.24845	1.223	2209.96
3	CCSD(T)/aug-cc-pVTZ	−498.25976	−498.21423	−498.20422	1.239	2196.94
4	CCSD(T)/aug-cc-pVQZ	−498.28958	−498.24347	−498.23334	1.255	2223.28
5	CCSD(T)/aug-cc-pV5Z	−498.29937	−498.25339	−498.24334	1.251	2205.72
∞	CBS-3parameter	−498.30506	−498.25916	−498.24909	1.249	2195.20
Expt.					1.210 ± 0.005[a]	2163.28 ± 0.05[c]
Expt.					1.213 ± 0.005[b]	2169.06 ± 0.10[d]

[a] Ref. [41].
[b] Ref. [40].
[c] Ref. [23].
[d] Ref. [35].

3. Computational

Geometry optimization and frequency calculations have been carried out on the $\tilde{X}^2A''$ state of $HCCl^-$ and the $\tilde{X}^1A'$ and $\tilde{a}^3A''$ states of HCCl by the CCSD(T) theory with the Dunning's correlation consistent basis sets, which were performed on the GAUSSIAN09 program package [56].

The Franck–Condon factors calculations on the $HCCl(\tilde{X}^1A')$–$HCCl^-(\tilde{X}^2A'')$ and $HCCl(\tilde{a}^3A'')$–$HCCl^-(\tilde{X}^2A'')$ photodetachments have been explored, utilizing the CCSD(T) force constants and structural parameters for the initial electronic state

$\tilde{X}^2A''$ of $HCCl^-$ and the final electronic states $\tilde{X}^1A'$ and $\tilde{a}^3A''$ of HCCl. It's worth noting that the Franck–Condon analysis procedure and the spectral simulation method applied in the present paper on the basis of the harmonic oscillator model and considering Duschinsky effects, which have been described in Section 2. Then the calculated FCFs were utilized to simulate the vibrational structures of the singlet and triplet transitions of $HCCl^-$, utilizing a Gaussian line shape and a full-width-at-half-maximum (FWHM) of 340 cm^{-1}.

The energy at the CBS limit (E_{CBS}) was obtained by fitting the calculated energies to a three-parameter mixed exponential/Gaussian function [43] of the form:

$$E(l) = E_{CBS} + B\exp[-(l-1)] + C\exp\left[-(l-1)^2\right] \quad (4)$$

where l refers to the maximum angular momentum quantum number in the basis set and E_{CBS} is the energy extrapolated to the basis set limit. For the cc-pVTZ/aug-cc-PVTZ, cc-pVQZ/aug-cc-PVQZ and cc-pV5Z/aug-cc-PV5Z basis sets, l = 3–5, respectively, and B and C are adjustable parameters.

4. Results and analysis

4.1. Equilibrium structural parameters and harmonic vibrational frequencies

The equilibrium structural parameters and harmonic vibrational frequencies for the $\tilde{X}^2A''$ state of $HCCl^-$ and the $\tilde{X}^1A'$ and $\tilde{a}^3A''$ states of HCCl have been shown in Tables 1–3. As a comparison, both the experimental data and theoretical values available in the related references are also exhibited. According to the convention of triatomic molecules, the ω_1, ω_2 and ω_3 are the C—H stretch, H—C—Cl bending and C—Cl stretch vibrational frequencies, respectively [55,57–59].

According to Table 1, the bond lengths, bond angles and harmonic vibrational frequencies acquired at the different levels of calculation seem to be highly consistent, which are in extremely agreement with the corresponding available calculated and observed data. For R(C—H), R(C—Cl) and ∠HCCl of $HCCl^-$, the theoretically calculated values compared with the experimental results [41], the maximum errors between them are less than 0.0216 Å, 0.0841 Å and 5.25°, respectively. In Ref. [41], the anion geometries are derived from Franck–Condon analysis of the PES of $HCCl^-$ based on the geometry of $\tilde{X}^1A'$ HCCl determined by Kakimoto et al. [29]. The geometric parameters from Hirota's work carry significant uncertainties, which are necessarily transferred onto the anion geometric parameters through the Franck–Condon analysis. Furthermore, the Franck–Condon analysis by Lineberger and coworkers itself adds significant uncertainties to the anion geometric parameters. In addition, Lineberger and coworkers used Hirota's geometric values in their Franck–Condon analysis while the present study derived geometric values in our quantum chemical computations. The values of bond lengths and bond angles of $HCCl^-$ on the basis of theoretical calculation at the CCSD(T)/aug-cc-pV5Z level of theory are 1.1184 Å, 1.8982 Å and 96.98°. For R(C—H), R(C—Cl) and ∠HCCl of the $HCCl^-$ anion, the distinctions between calculated values and experimental data are only 0.0216 Å, 0.0118 Å and 2.52°, respectively. As mentioned above, both the vibrational frequencies and optimized structural parameters of $HCCl^-$ anion gained at the CCSD(T)/aug-cc-pV5Z method have shown a good agreement with the available calculated and experimental data in Table 1, and therefore were exploited in the later iterative Franck–Condon analysis and spectral simulations.

For the $\tilde{X}^1A'$ and $\tilde{a}^3A''$ states of HCCl, the bond lengths, bond angles and vibrational frequencies computed at CCSD(T) level with different basis sets are extremely consistent in Tables 2 and 3. The computed values compared well with other theoretical and experimental studies included in the tables. In Table 2, for the $\tilde{X}^1A'$ state of HCCl, the maximum differences between experimental and theoretical bond lengths and bond angles are less than 0.0218 Å, 0.0441 Å and 3.74° for R(C—H), R(C—Cl) and ∠HCCl, respectively. The calculated values of HCCl based on quantum chemical computations at the CCSD(T)/aug-cc-pV5Z level are 1.1082 Å, 1.6927 Å and 102.27°. And the variances between the experimental and theoretical data are only 0.0218 Å, 0.0057 Å and 2.83° for R(C—H), R(C—Cl) and ∠HCCl, respectively. In Table 3, the computed structures and harmonic vibrational frequencies of the $\tilde{a}^3A''$ state of HCCl derived at CCSD(T) calculations are seen to be extremely coherent. Considering no experimentally measured structural parameters for comparison, the values obtained at the higher level method should be the more dependable and therefore the CCSD(T)/aug-cc-pV5Z results were employed in the next spectral simulations.

4.2. Single point energy, electron affinity and term energy of HCCl

The single point energy (SPE), electron affinity (EA) and term energy (TE) at the CCSD(T) level of theory have been shown in Table 4: EA = SPE (neutral singlet)–SPE (anion) and TE = SPE (neutral triplet)–SPE (neutral singlet). The theoretical and/or experimental values available in the literature are also included for comparison. From Table 4, it is clear that the computed EA and TE values obtained in this work at different levels of calculation are very consistent. It is also noteworthy that the values are deeply influenced by whether the Dunning's correlation consistent basis sets involving augmented correlated consistent polarized valence. For example, the values of EA calculated by CCSD(T) method with the cc-pVTZ and aug-cc-pVTZ basis sets are 1.239 eV and 0.914 eV, the difference between them is 0.325 eV. With the increase of basis sets, the difference becomes smaller. However, there is still a 0.074 eV variance between the CCSD(T)/cc-pV5Z and CCSD(T)/aug-cc-pV5Z values. It can be concluded that the basis sets involving the augmented correlated consistent polarized valence are important to EA. The EA values estimated at the CCSD(T) theory level with the aug-cc-pVTZ, aug-cc-pVQZ and aug-cc-pV5Z basis sets are 1.239, 1.255 and 1.251 eV, respectively, which are in agreement with the experimental results. Furthermore, the energies obtained at the complete basis set limit are 1.223 eV and 1.249 eV, respectively, at the CCSD(T) level with cc-pVXZ and aug-cc-pVXZ basis sets by a three-parameter mixed exponential/Gaussian function, which are in rather agreement with other observed and theoretical values shown in Table 4.

For the TE of HCCl, the largest deviations between the experimental [35], and theoretical values are less than 121.36 cm^{-1} in this work, suggesting that they are reliable. The best estimation of the term energy is 2195.20 cm^{-1}, which was obtained at the CCSD(T) level with aug-cc-pVXZ basis set to be extrapolated to the complete basis set limit on the basis of the three-parameter mixed exponential/Gaussian function. The value is in excellent agreement with the experimental measurement of 2169.06(10) cm^{-1} [35] for the term energy of HCCl.

4.3. Mode mixing effects and geometrical displacement

On the basis of GAUSSIAN09 output, the Duschinsky matrix **J** and displacement vector **K** for the transition between two different electronic states are given [51]

$$\mathbf{J} = [\mathbf{M}(\mathbf{g09}')\mathbf{V}'^{-1/2}]^{\dagger}\mathbf{Z}(\mathbf{g09})\mathbf{V}^{-1/2} \text{and} \mathbf{K} = [\mathbf{M}(\mathbf{g09}')\mathbf{V}'^{-1/2}]^{\dagger}\mathbf{R} \quad (5)$$

where, normally, unprimed and primed quantities involve in the initial and final states separately. In Eq. (5), some matrix and vectors involved are defined in Ref. [51].

For the $HCCl^-(\tilde{X}^2A'')$–$HCCl(\tilde{X}^1A')$ electronic transition, the Duschinsky matrix **J** and displacement vector **K** evaluated at the CCSD(T)/aug-cc-pV5Z theory level are as follows:

$$\mathbf{J}^1 = \begin{bmatrix} 0.98 & 0.10 & 0.02 \\ -0.11 & 0.99 & -0.01 \\ -0.02 & 0.03 & 1.01 \end{bmatrix}, \mathbf{K}^1 = \begin{bmatrix} 0.06 \\ 0.07 \\ 2.26 \end{bmatrix} \quad (6)$$

where $\mathbf{K}^1$ are in units of amu$^{1/2}$ Å and $\mathbf{J}^1$ describe the mixing of normal modes, reveal that each one of the three a' modes of $HCCl^-$, map on to a linear combination of the three a' modes of HCCl ($\tilde{X}^1A'$). Each column in $\mathbf{J}^1$ is normalized and the sum of the squares of the mixing coefficients adding up to unity within rounding errors. The mode mixing matrix $\mathbf{J}^1$ shows that there is some, albeit not large ($J^1_{12} = 0.10$, $J^1_{13} = 0.02$, $J^1_{23} = -0.01$), Duschinsky effect between $\omega_1(a')$, $\omega_2(a')$ and $\omega_3(a')$ vibrational modes. The normal coordinate displacement $\mathbf{K}^1$ from the anion to the neutral ($\tilde{X}^1A' \longleftarrow \tilde{X}^2A''$) are $\Delta Q^1_1 = 0.06$, $\Delta Q^1_2 = 0.07$ and $\Delta Q^1_3 = 2.26$ which means that the bond length R(C—H) diminishes, the bond angle ∠HCCl increases and the bond length R(C—Cl) decreases, respectively. Meanwhile, one can observe that ΔQ^1_3 is much larger than $\Delta Q^1_1/\Delta Q^1_2$, derived from the big variation of the bond length R(C—Cl), and thus a long progression of the stretching vibration (ω_3) transition is shown in the $\tilde{X}^1A' \longleftarrow \tilde{X}^2A''$detachment spectrum of $HCCl^-$ (see the spectral simulation below).

For the $HCCl^-$ ($\tilde{X}^2A''$)–HCCl ($\tilde{a}^3A''$) electronic transition, the Duschinsky matrix **J** and displacement vector **K** calculated at the CCSD(T)/aug-cc-pV5Z theory level are as follows:

$$\mathbf{J}^2 = \begin{bmatrix} -0.87 & 0.47 & -0.02 \\ 0.47 & 0.84 & -0.23 \\ 0.07 & -0.22 & 0.97 \end{bmatrix}, \mathbf{K}^2 = \begin{bmatrix} 0.16 \\ 2.97 \\ 1.85 \end{bmatrix} \quad (7)$$

The normal mode mixing matrix $\mathbf{J}^2$ shows that there is large Duschinsky effect between $\omega_1(a')$ and $\omega_2(a')$ vibrational modes ($J^2_{12} = 0.47$), whereas vibrational modes $\omega_1(a')$ coupled from $\omega_3(a')$ is small ($J^2_{13} = -0.02$). From the anion to the neutral ($\tilde{a}^3A'' \longleftarrow \tilde{X}^2A''$), the matrix elements of $\mathbf{K}^2$ are $\Delta Q^2_1 = 0.16$, $\Delta Q^2_2 = 2.97$and $\Delta Q^2_3 = 1.85$, respectively, which correspond to the bond length R(C—H) decrease, the bond angle∠HCCl increase and the bond length R(C—Cl) decrease, respectively. Furthermore, one can observe that $\Delta Q^2_2/\Delta Q^2_3$ is much larger than ΔQ^2_1, due to the large changes of the bond length R(C—Cl) and the bond angle ∠HCCl, and therefore long combining progressions of the bending vibration (ω_2) and the stretching vibration (ω_3) transitions are expected in the $\tilde{a}^3A''$–$\tilde{X}^2A''$ detachment spectrum of $HCCl^-$ (see the results of the spectral simulation below).

4.4. Comparison between observed and calculated PES of $HCCl^-$

We focus on the photoelectron spectroscopy of $HCCl^-$ for the $\tilde{X}^1A'$–$\tilde{X}^2A''$ and $\tilde{a}^3A''$–$\tilde{X}^2A''$ detachments by utilizing force constants and geometries obtained on the CCSD(T)/aug-cc-pV5Z level. The simulated stick diagrams of the $\tilde{X}^1A'$–$\tilde{X}^2A''$ and $\tilde{a}^3A''$–$\tilde{X}^2A''$ are shown in Fig. 1a and b, respectively. Then we have merged the two detachments together, and the stick diagrams and the simulated spectra with a FWHM of 340 cm^{-1} and a Boltzmann vibrational temperature of 270 K which are shown in Fig. 1c (including hot band). Furthermore, the simulated spectra and the experimental one are shown in Fig. 2 for comparison [41].

For the $\tilde{X}^1A'$–$\tilde{X}^2A''$ detachment of $HCCl^-$ anion vibration assignments, the C—Cl stretching mode ω_3 is involved in Fig. 1a and the label (0, 0, 0)–(0, 0, n) for the assignment means the transition (0, 0, 0)–(0, 0, ω_3). We found that in the spectral simulation, the FCFs for the photo-detachment process including the C—H stretching mode ω_1 and the bending mode ω_2 are almost negligible. However, vibration assignments for the $\tilde{a}^3A''$–$\tilde{X}^2A''$ of $HCCl^-$, the bending mode ω_2 and C—Cl stretching mode ω_3 are involved in Fig. 1b. With labels (0, 0, 0)–(0, n, 0), (0, 0, 0)–(0, n, 1) and (0, 0, 0)–(0, n, 2) corresponding to the (0, 0, 0)–(0, ω_2, ω_3) transition. It has been found that the bending mode ω_2 and C—Cl stretching mode ω_3 plays a major role, while C—H stretching mode ω_1 plays a secondary effect in the spectral simulation and almost negligible. After consideration of vibrational assignments for the $\tilde{X}^1A'$–$\tilde{X}^2A''$ and $\tilde{a}^3A''$–$\tilde{X}^2A''$ detachments, respectively, the two transitions were merged together. Only in this way would we acquire a good agreement between the theoretical and experimental spectra, which are shown in Fig. 2.

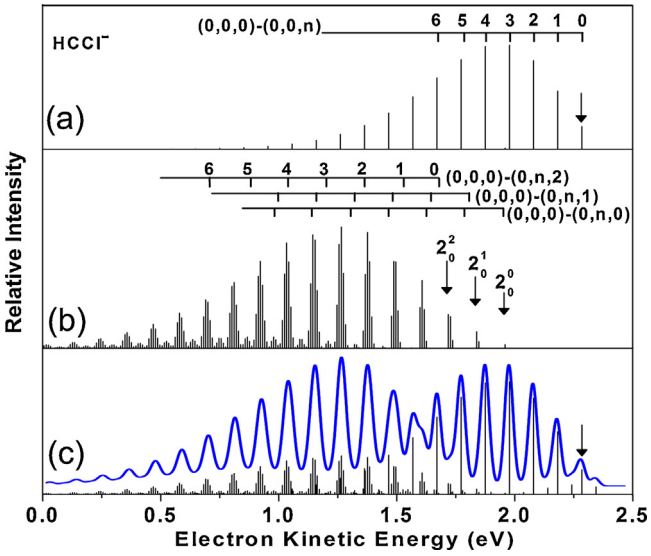

Fig. 1. The calculated photoelectron spectra of $HCCl^-$ obtained at a Boltzmann vibrational temperature of 270 K. (a) The calculated stick diagram with vibrational assignment provided for the $\tilde{X}^1A'$–$\tilde{X}^2A''$ detachment process, and (b) the calculated stick diagram with vibrational assignments provided for the $\tilde{a}^3A''$–$\tilde{X}^2A''$ detachment process, and (c) calculated photoelectron spectra with vibrational assignments involved the $\tilde{X}^1A'$–$\tilde{X}^2A''$ and $\tilde{a}^3A''$–$\tilde{X}^2A''$ detachment processes and with a FWHM of 340 cm^{-1} (including hot band).

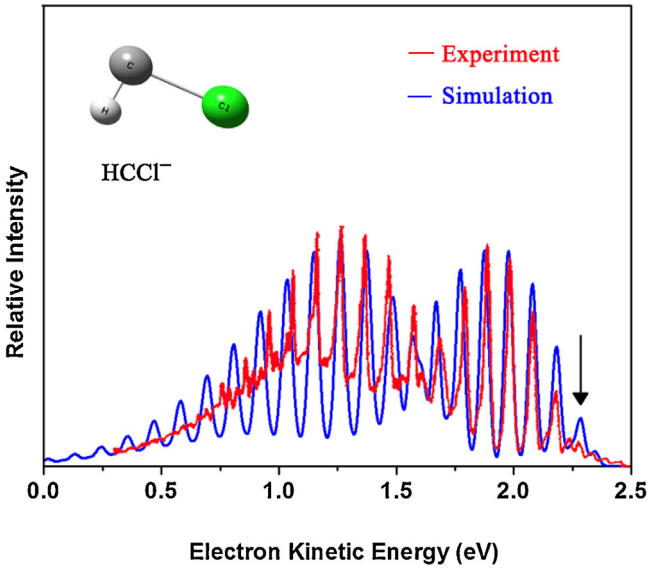

Fig. 2. The observed photoelectron spectra of $HCCl^-$ obtained from Ref. [41] (red line), the simulated spectra with vibrational assignments provided for the $\tilde{X}^1A'$–$\tilde{X}^2A''$ and $\tilde{a}^3A''$–$\tilde{X}^2A''$ detachment processes with a FWHM of 340 cm^{-1} and a Boltzmann vibrational temperature of 270 K (blue line). (For interpretation of the references to color in this figure legend, the reader is referred to the web version of this article.)

From Fig. 2, the results show that the computed photoelectron spectra are rather identical to the observed one. This means the CCSD(T)/aug-cc-pV5Z geometry changes for the $\tilde{X}^1A'$, $\tilde{X}^2A''$ and $\tilde{a}^3A''$ electronic states are reasonably precise, and harmonic oscillator model used ought to be relatively approximate. However, we have found that the relative intensity of the two different electronic transitions from the ground vibrational state of the anion to different vibrational levels of the neutrals between simulation and observation there are always deviations, and the deviations added with the increase of the vibrational quantum numbers. The deviations are results of the anharmonicity effects not considered in the Franck–Condon Factors analysis and have also been observed previously in other molecules [60,61]. Tarczay et al. have performed VPT2 and variational calculations for HCCl on the basis of the quartic force fields derived from CCSD(T)/aug-cc-pVQZ calculations and also shown the highly excited vibrational levels of HCCl has significant (>15 cm^{-1}) inaccuracy from the experimental results [10]. Another, in the $\tilde{X}^1A'$ state of HCCl, Renner–Teller effects shift levels and with a K-dependence leading to anharmonically spaced bending levels [17,26]. With the increase of the quantum numbers, these effects have become increasingly evident and the impacts on the theoretical spectra become progressively stronger.

5. Summary

Geometry optimization and frequency calculations have been performed on the $\tilde{X}^2A''$ state of $HCCl^-$, and the $\tilde{X}^1A'$ and $\tilde{a}^3A''$ states of HCCl at the CCSD(T) method. The electron affinity and term energy of HCCl were computed at the CCSD(T) level with Dunning's correlation consistent basis sets and to be extrapolated to the complete basis set limit. We have simulated the observed PES of the $HCCl(\tilde{X}^1A')$–$HCCl^-(\tilde{X}^2A'')$ and $HCCl(\tilde{a}^3A'')$–$HCCl^-(\tilde{X}^2A'')$ transitions employing a harmonic model and considering Duschinsky effects. The theoretical spectra and experimental one are in good agreement. Hence, we concluded that the geometry parameters of $HCCl^-$ obtained at the CCSD(T)/aug-cc-pV5Z level of theory are extremely precise and the harmonic oscillator model ought to be reasonably adequate.

Acknowledgments

This work was supported by the National Nature Science Foundation of China (No. 21273009), the Nature Science Foundation of the Education Committee of Anhui (No. KJ2009A131), the Program for Innovative Research Team in Anhui Normal University and the Doctoral Research Foundation of Anhui Normal University (No. 750706).

References

[1] V. Loukonen, I.F.W. Kuo, M.J. McGrath, H. Vehkamaki, Chem. Phys. 428 (2014) 164.
[2] F. Atash, Cities 24 (2007) 399.
[3] I.K. Ortega, O. Kupiainen, T. Kurtén, T. Olenius, O. Wilkman, M.J. McGrath, V. Loukonen, H. Vehkamäki, Atmos. Chem. Phys. 12 (2012) 225.
[4] Y. Xu, A.B. Nadykto, F. Yu, J. Herb, W. Wang, J. Phys. Chem. A 114 (2010) 387.
[5] I.M. Kennedy, Proc. Combust. Inst. 31 (2007) 2757.
[6] G.E. Scuseria, M. Duran, R. Maclagan, H.F. Schaefer, J. Am. Chem. Soc. 108 (1986) 3248.
[7] M.L. McKee, J. Org. Chem. 62 (1997) 7942.
[8] M. Schwartz, P. Marshall, J. Phys. Chem. A 103 (1999) 7900.
[9] K. Sendt, T.W. Schmidt, G.B. Bacskay, Int. J. Quantum Chem. 76 (2000) 297.
[10] G. Tarczay, T.A. Miller, G. Czako, A.G. Csaszar, Phys. Chem. Chem. Phys. 7 (2005) 2881.
[11] G. Tarczay, T.A. Miller, G. Czako, A.G. Csaszar, Phys. Chem. Chem. Phys. 10 (2008) 7324.
[12] H.G. Yu, T.J. Sears, J.T. Muckerman, Mol. Phys. 104 (2006) 47.
[13] J. Zhang, J. Ma, Z. Wang, Chem. Phys. Lett. 546 (2012) 47.
[14] J. Liang, Y. Wang, Z. Geng, G. Li, Y. Wei, Struct. Chem. 24 (2013) 455.
[15] J. Liang, Q. Su, S. Zheng, J. Yu, Z. Geng, J. Theor. Comput. Chem. 14 (2015) 1550009.
[16] C.W. Bauschlicher, H.F. Schaefer, P.S. Bagus, J. Am. Chem. Soc. 99 (1977) 7106.
[17] B.C. Chang, T.J. Sears, J. Chem. Phys. 102 (1995) 6347.
[18] C.L. Lee, M.L. Liu, B.C. Chang, J. Chem. Phys. 117 (2002) 3263.
[19] C.S. Lin, Y.E. Chen, B.C. Chang, J. Chem. Phys. 121 (2004) 4164.
[20] C. Tao, C. Mukarakate, S.A. Reid, J. Chem. Phys. 124 (2006) 224314.
[21] S.K. Shin, P.J. Dagdigian, J. Chem. Phys. 128 (2008) 064309.
[22] T.C. Steimle, F. Wang, X. Zhuang, Z. Wang, J. Chem. Phys. 136 (2012) 114309.
[23] C. Tao, C. Mukarakate, Z. Terranova, C. Ebben, R.H. Judge, S.A. Reid, J. Chem. Phys. 129 (2008) 104309.
[24] S.H. Kable, S.A. Reid, T.J. Sears, Int. Rev. Phys. Chem. 28 (2009) 435.
[25] S.K. Shin, P.J. Dagdigian, Phys. Chem. Chem. Phys. 8 (2006) 3446.
[26] S.K. Shin, P.J. Dagdigian, J. Chem. Phys. 125 (2006) 133317.
[27] A.J. Merer, D.N. Travis, Can. J. Phys. 44 (1966) 525.
[28] M.E. Jacox, D.E. Milligan, J. Chem. Phys. 47 (1967) 1626.
[29] M. Kakimoto, S. Saito, E. Hirota, J. Mol. Spectrosc. 97 (1983) 194.
[30] B.C. Chang, T.J. Sears, J. Mol. Spectrosc. 173 (1995) 391.
[31] B.C. Chang, R.A. Fei, T.J. Sears, J. Mol. Spectrosc. 183 (1997) 341.
[32] C.W. Chen, T.C. Tsai, B.C. Chang, Chem. Phys. Lett. 347 (2001) 73.
[33] H. Fan, I. Ionescu, C. Annesley, J. Cummins, M. Bowers, S.A. Reid, J. Mol. Spectrosc. 225 (2004) 43.
[34] Z. Wang, R.G. Bird, H.G. Yu, T.J. Sears, J. Chem. Phys. 124 (2006) 074314.
[35] C. Tao, C. Mukarakate, R.H. Judge, S.A. Reid, J. Chem. Phys. 128 (2008) 171101.
[36] R. Hoffmann, G.D. Zeiss, G.W. Vandine, J. Am. Chem. Soc. 90 (1968) 1485.
[37] K. Sendt, G.B. Bacskay, J. Chem. Phys. 112 (2000) 2227.
[38] A.P. Scott, M.S. Platz, L. Radom, J. Am. Chem. Soc. 123 (2001) 6069.
[39] A. Lin, K. Kobayashi, H.G. Yu, G.E. Hall, J.T. Muckerman, T.J. Sears, A.J. Merer, J. Mol. Spectrosc. 214 (2002) 216.
[40] K.K. Murray, D.G. Leopold, T.M. Miller, W.C. Lineberger, J. Chem. Phys. 89 (1988) 5442.
[41] M.K. Gilles, K.M. Ervin, J. Ho, W.C. Lineberger, J. Phys. Chem. 96 (1992) 1130.
[42] F. Duschinsky, Acta Physicochim. URSS 7 (1937) 551.
[43] K.A. Peterson, D.E. Woon, T.H. Dunning, J. Chem. Phys. 100 (1994) 7410.
[44] I. Ozkan, J. Mol. Spectrosc. 139 (1990) 147.
[45] T.E. Sharp, H.M. Rosenstock, J. Chem. Phys. 41 (1964) 3453.
[46] R. Berger, C. Fischer, M. Klessinger, J. Phys. Chem. A 102 (1998) 7157.
[47] K.M. Ervin, T.M. Ramond, G.E. Davico, R.L. Schwartz, S.M. Casey, W.C. Lineberger, J. Phys. Chem. A 105 (2001) 10822.
[48] A.V. Sergeev, B. Segev, J. Chem. Phys. 118 (2003) 5852.
[49] C.L. Lee, S.H. Yang, S.Y. Kuo, J.L. Chang, Mol. Phys. 256 (2009) 279.
[50] V. Barone, J. Bloino, M. Biczysko, F. Santoro, J. Chem. Theory Comput. 5 (2009) 540.
[51] J. Liang, C. Liu, C. Wang, Z. Cui, Mol. Phys. 107 (2009) 2601.
[52] F. Santoro, V. Barone, Int. J. Quantum Chem. 110 (2010) 476.
[53] J. Bloino, M. Biczysko, F. Santoro, V. Barone, J. Chem. Theory Comput. 6 (2010) 1256.
[54] J. Liang, R. Wang, X. Liang, Y. Liu, C. Pan, F. Yang, Z. Cui, Mol. Phys. 109 (2011) 1727.
[55] J. Liang, F. Cui, R. Wang, W. Huang, Z. Cui, J. Mol. Spectrosc. 286 (2013) 12.
[56] M. Frisch, G. Trucks, H. Schlegel, G. Scuseria, M. Robb, J. Cheeseman, G. Scalmani, V. Barone, B. Mennucci, G. Petersson, Gaussian 09, Gaussian Inc., Wallingford, CT, 2009.
[57] R. Li, X. Zhang, H. Zheng, J. Liang, Z. Cui, J. Mol. Struct.: THEOCHEM 860 (2008) 106.
[58] J. Liang, H. Zheng, X. Zhang, R. Li, Z. Cui, J. Mol. Struct.: THEOCHEM 814 (2007) 99.
[59] J. Liang, H.Y. Li, J. Electron Spectrosc. Relat. Phenom. 135 (2004) 119.
[60] J. Liang, X.L. Kong, X.Y. Zhang, H.Y. Li, Chem. Phys. 294 (2003) 85.
[61] H. Zheng, X. Zhang, R. Li, J. Liang, Z. Cui, Chem. Phys. Lett. 448 (2007) 178.